

Combining commercial microwave links and weather radar for classification of dry snow and rainfall

Erlend Øydvin¹, Renaud Gaban^{1,5}, Jafet Andersson², Remco (C. Z.) van de Beek², Mareile Astrid Wolff^{1,5}, Nils-Otto Kitterød⁴, Christian Chwala³, and Vegard Nilsen¹

¹Faculty of Science and Technology, Norwegian University of Life Sciences, Ås, Norway

²Swedish Meteorological and Hydrological Institute (SMHI), 601 76 Norrköping, Sweden

³Institute of Meteorology and Climate Research, Karlsruhe Institute of Technology, Campus Alpin, Garmisch-Partenkirchen, Germany

⁴Faculty of Environmental Sciences and Natural Resource Management, Norwegian University of Life Sciences, Ås, Norway

⁵Norwegian Meteorological Institute, Oslo, Norway

Correspondence: Erlend Øydvin (erlend.oydvin@nmbu.no)

Abstract. Differentiating between snow and rainfall is crucial for hydrological modeling and understanding. Commercial Microwave Links (CMLs) can provide ~~accurate~~-rainfall estimates for liquid precipitation, but show minimal signal attenuation during dry snow events, causing the CML time series during these periods to resemble non-precipitation periods. Weather radars can detect precipitation also for dry snow, yet ~~they~~ struggle to accurately differentiate between precipitation types.

- 5 This study introduces a new approach to improve rainfall and dry snow classification by combining weather radar precipitation detection with CML signal attenuation. Specifically, events where the radar detects precipitation, but the CML does not, are classified as dry snow. As a reference method, we use weather radar ~~with~~ the precipitation type identified by the dew point temperature at the CML location. Both methods were evaluated using ~~ground~~-measurements from disdrometers located within 8 km of a CML, ~~analysing data from taken as ground truth. The analysis used data from Norway, including~~ 550 CMLs in
- 10 December 2021 and 435 CMLs in June 2022. Our results show that ~~using CMLs can enhance the use of CMLs can improve~~ the classification of dry snow and rainfall, presenting an advantage over the reference method. ~~Further~~In addition, our research provides valuable ~~insights~~insight into how precipitation at temperatures around zero degrees, such as sleet or wet snow, can affect CMLs, contributing to a better understanding of CML applications in colder climates.

1 Introduction

- 15 The precipitation phase is crucial for hydrological processes in cold regions (Loth et al., 1993). Understanding the type of precipitation aids in applications such as adjusting rain gauges for wind undercatch (Kochendorfer et al., 2022) and modeling hydrological responses ~~like~~such as flooding. Moreover, specific precipitation conditions, like freezing rain, can disrupt power lines and impede traffic, ~~while snow can and snow may~~ cause transportation blockages. ~~It's also noteworthy that rain-on-snow events have~~Rain-on-snow events have also been associated with significant flooding (McCabe et al., 2007), and with slush
- 20 avalanches (Hestnes, 1985).

The formation of precipitation is a complex process. In the high and mid-latitudes, most precipitation originates from mixed-phase or cold clouds, ~~i.e. that is~~ clouds containing ice (Stewart et al., 2015). The ice crystals grow in size and mass through different micro-physical mechanisms such as vapor deposition and riming, until they reach a sufficient mass to sediment out of the cloud base (Stewart, 1992). A necessary condition for a cloud to generate solid phase-precipitation is that its temperature is negative. Unless the temperature of the layer of atmosphere underneath the cloud remains below zero degrees, the precipitating ice will start melting before reaching the ground (Lamb and Verlinde, 2011). The melting process is not instantaneous and an ice particle can fall hundreds of meters before melting completely. Therefore, originally solid precipitation can reach the ground in any intermediate state between solid and liquid, depending on the ~~height-elevation~~ of the zero-degree isotherm (Paulson and Al-Mreri, 2011; Harpold et al., 2017). The melting process is also influenced by other elements of the atmospheric conditions. Specifically, the stability of the atmosphere and the atmospheric humidity profile have a significant influence because the liquid water formed from melting of ice will tend to evaporate in dry conditions, cooling the atmosphere in turn and hampering further melting (Harder and Pomeroy, 2013). Atmospheric conditions that determine the precipitation phase can change relatively quickly. For instance, a study by Marks et al. (2013) observed a significant increase of the ~~height-elevation~~ of the melting layer within the same precipitation event. Determining the precipitation phase at the ground level is therefore difficult and models predicting the precipitation phase typically need to be calibrated and validated against measurements (Harpold et al., 2017).

There are several ways of determining the precipitation phase using ground based observations. For example, Marks et al. (2013) used a combination of a tipping bucket rain gauge and a heated weighing gauge. During rain, the devices record similar amounts, but when it snows, the snow clogs the funnel of the tipping bucket, leaving only the weighing gauge to record precipitation. Other studies, such as Matsuo et al. (1981), used human observers to directly observe precipitation phase. More advanced methods include using weather radars, especially with dual polarization, to estimate and classify precipitation phase (Grazioli et al., 2015; Chandrasekar et al., 2013). Disdrometers also estimate precipitation phase based on the physical properties of hydrometeors (size and fall velocity), with semi-empirical knowledge of how these properties vary with type (Löffler-Mang and Joss, 2000; Yuter et al., 2006). However, each method has its own limitations. Rain gauges, providing point measurements, have limited spatial representation and can be affected by ~~wind-induced-wind-induced~~ errors (Førland et al., 1996; Nešpor and Sevruk, 1999; Kochendorfer et al., 2022; Wolff et al., 2015). Human observations can be subjective and ~~aren't~~ ~~are not~~ suitable for continuous ~~high-frequency-monitoring. Dual-polarized-weather-radar-high-rate monitoring. Weather radars~~ can suffer from beam blockage ~~and has difficulty~~ (Berne and Krajewski, 2013), ~~overshooting, and still have difficulties~~ linking the estimated precipitation type to ground measurements (Harpold et al., 2017; Elmore, 2011). Like rain gauges, disdrometers are limited in spatial representation and can experience errors such as splashing of drops against nearby structures, drops falling on the edge of the measuring area, and wind altering ~~the~~ drop trajectories (Friedrich et al., 2013).

Precipitation phase estimation often employs a temperature model. This involves modeling the rain-snow transition based on temperature using for instance a single temperature threshold to separate rain and snow, or two thresholds that define mixed precipitation in between the two thresholds (Kienzle, 2008). Jennings et al. (2018) found that, when using a single temperature threshold, the threshold separating rain from snow varies geographically, ranging from -0.4 to 2.4 for most stations and with colder thresholds near the coast and warmer thresholds in mountains. They also found that models incorporating humidity

performed better than models considering air temperature alone, which is ~~also~~ confirmed by other studies (Matsuo et al., 1981). ~~Other studies again have not observed~~ Although some studies do not observe any benefit of including humidity (Leroux et al., 2023), humidity is thought to be an important parameter since the atmospheric moisture level affects the melting and evaporating precipitation, influencing whether precipitation reaches the ground as solid or liquid (Kuhn, 1987). One common
60 measure combining humidity and temperature is the dew point temperature, which is the temperature at which ~~air becomes~~ the air would become saturated with water vapor at ~~the current water constant pressure and moisture~~ content (Lawrence, 2005). ~~This measure can provide important insights into the atmospheric conditions and aids in classifying precipitation types (Feiccabrino, 2020; Harder and Pomeroy, 2013, 2014). However, even if temperature and humidity are combined to classify precipitation types, there is still~~ In a dry atmosphere, the dew point temperature is significantly lower than the air temperature.
65 In these conditions, melting is not favored and snow can be observed at positive air temperatures. Conversely, the dew point and the air temperatures are equal if the air is saturated, and solid precipitation will more likely have melted before reaching the ground if the air temperature is above 0 degrees (Feiccabrino, 2020; Harder and Pomeroy, 2013, 2014). However, a large degree of uncertainty in precipitation type classification remains even when temperature and humidity are combined. Harpold et al. (2017) suggest that current phase transition models are too simple to capture the process, especially in complex terrain.
70 They suggest, for instance, to improve this by better use of other atmospheric information and enhancing the validation network with ground measurements such as disdrometers.

CMLs Commercial microwave links (CMLs) are radio links between radio communication towers. In the mid-2000s, it was demonstrated by Messer et al. (2006) and Leijnse et al. (2007) that CMLs can be used to estimate rainfall. This is due to the relationship between signal attenuation and rainfall intensity. At around 30 GHz, the relation is close to linear, making it easier
75 to estimate the average rainfall intensity along the CML path. Among other applications, CMLs have been used to estimate countrywide rainfall (Graf et al., 2020; Overeem et al., 2016), transboundary rainfall fields (Blettner et al., 2023) and CMLs have proven useful for estimating runoff in urban hydrology (Pastorek et al., 2023). A crucial step in CML rainfall estimation is the detection of rainfall, often called wet periods, in the CML time series. There are several ways of doing this, for instance by classifying a period as wet when the standard deviation of a moving window is larger than a predefined threshold (Schleiss
80 et al., 2013; Graf et al., 2020), by using pre-trained classification ~~methods-models~~ (Polz et al., 2020; Øydvin et al., 2024) or by including information from nearby CMLs ~~(Overeem et al., 2013)~~ (Overeem et al., 2011). It is also possible to use weather radar to estimate the CML wet period as done in Overeem et al. (2016).

Classification of precipitation types other than rain using CMLs has previously been investigated by Cherkassky et al. (2014). The authors used the fact that snow, sleet (defined as a mixture of snow and rain), and rainfall are affected differently
85 by different CML frequencies. Thus, by using three CMLs operating at different frequencies in the same area, they were able to distinguish periods of ~~wet snow-sleet~~ and rainfall, albeit only for two precipitation events ~~where each lasted for~~, each lasting three days. Ostrometzky et al. (2015) expanded on this study by using four CMLs operating at different frequencies and clustered at a single path to estimate the precipitation amounts generated by rainfall and ~~wet snowsleet~~. The study investigated four precipitation events lasting a total of 16 days. A limitation of both of these studies is that they focus on a low number of
90 CMLs over a few days. It is not known how well these methods generalize to longer time series and larger CML networks.

Not many Other studies have focused on how CMLs are affected by colder climates. Hansryd et al. (2010) reported that heavy snowfall caused minimal signal attenuation, while a mix of rain and snow, caused higher signal attenuation. van Leth et al. (2018) observed that during an event with a mixed precipitation the CMLs experience a strong signal attenuation which persisted for about 10 minutes after the precipitation event, possibly due to melting of snow off from the antenna cover. Graf et al. (2020) and Overeem et al. (2016) reported that CMLs tend to overestimate the precipitation amount during winter months. Both attributed this overestimation to wet snow. Paulson and Al-Mreri (2011) reports that wet snow can induce melting snow, which is known to cause up to four times the attenuation compared to rainfall, leading to potential overestimation of CML rainfall due to the larger size of the wet snow particles depending on the mixture of snow and rain (Paulson and Al-Mreri, 2011). Dry snow, on the other hand, is known to cause signal attenuation so low that it cannot be detected by CMLs (Pu et al., 2020) (Pu et al., 2020; Paulson and Al-Mreri, 2011; Hansryd et al., 2010).

In this study, we explore the viability of classifying dry snow by exploiting the fact that dry snow causes unnoticeable attenuation in the CML data. This is done by first using the weather radar to detect precipitation and then classifying the precipitation type is classified based on whether the CML detects rainfall or not. We compare these estimates to ground truth observations from disdrometers operated by the road authorities in Norway, as well as a reference method that uses weather radar and dew point temperature to estimate the precipitation phase.

2 Methods

2.1 CML data

The CML dataset was provided by Ericsson and consists of 2777 CMLs spread out across Norway. Each CML records the transmitted and received signal strength every minute for data from two months: December 2021 and June 2022. The CML signal attenuation, often called total loss (TL), was computed by subtracting the received signal strength from the transmitted signal strength. In our dataset, there were some outliers where the transmitted signal strength was less than -50 dBm. These signals produced negative TL values, which is probably likely due to recording errors. We opted to completely remove CMLs with transmitted signal strength less than -50 dBm such that the remaining CMLs did not have any negative TL values. We also removed CMLs with more than 15% missing values. This resulted in 2179 CMLs for the summer dataset and 2345 CMLs from for the winter dataset. Next, as suggested by Graf et al. (2020), we removed erratic CMLs where the 5 hours moving window standard deviation exceeded the threshold of 2 dBm more than 10 % of the month and noisy CMLs where the 1-hour moving window standard deviation exceeded the threshold of 0.8 dBm more than 33 % of the month. Then CML derived rain rates were estimated using the pycomlink software (Chwala et al., 2023) and a similar workflow as described in Graf et al. (2020), Blettner et al. (2023) and Polz et al. (2020). For the classification of wet rainy periods, we used a simple feed-forward the convolutional neural network (MLP) available from pycomlink and described in Øydvin et al. (2024). To account for spatial and temporal differences between the CML and disdrometers, wet periods were extended by 5 minutes forward and 5 minutes backwards in time. Then, a constant baseline for each wet period CNN developed by Polz et al. (2020), as this model was trained on hourly data and this study also evaluates estimates at an hourly resolution. The baseline was estimated by using the average value of

the signal attenuation 5 dry-time steps before minutes before a rainy period. Water droplets forming on the antenna cover cause additional attenuation, which we accounted for by using the wet periods and the attenuation due to rain and wet antenna was estimated by subtracting the baseline attenuation from the TL. The attenuation caused by wet antennas was estimated using the method proposed by Leijnse et al. (2008) using the parameters obtained by Graf et al. (2020) semi-empirical wet antenna attenuation model proposed by Leijnse et al. (2008), with the refined parameters suggested by Graf et al. (2020). Finally, the rainfall rate was computed using the k-R relation, with parameters defined by ITU (2005) ITU (2005).

130 2.2 Radar data

Weather radar data for Norway was downloaded from THREDDS (2024), a data hosting platform for gridded meteorological data run by the Norwegian Meteorological Institute. The radar product is developed from 12 weather radars in Norway. These radars are combined using a Constant Altitude Plan Position Indicator (CAPPI). The final result is a grid with a spatial resolution of 1 km by 1 km and a temporal resolution of 5 minutes. Seaclutter and other large peaks in the data are removed, and groundclutter is identified and corrected using surrounding data. The radar reflectivity (Z [dBZ]) is converted to rainfall precipitation rates (R [mm/h]) using the Marshall-Palmer relation (Marshall and Palmer, 1948). To make the comparison of the CML and weather radar data consistent, we used the CML geometry to extract the average radar rainfall rate along the CML using a Radar precipitation rates were estimated along all CMLs using the weighted grid approach provided by *pycomlink*. Then, in line with Polz et al. (2020), time steps with weather radar rainfall rates above 0.1 mm/h were considered wet. To account for spatial and temporal differences between the radar beam and the disdrometer, periods with precipitation as detected by the weather radar were extended by 5 minutes forward and 5 minutes backward in time, similar to what was done with the CML wet periods. rainy.

2.3 Disdrometer data and co-located CMLs

As reference data for the true ground truth for the precipitation type, we used disdrometer data from the Norwegian road authorities. They use two types of disdrometers, namely the OTT Parsivel and OTT Parsivel². The disdrometer data was downloaded from Frost (2024), a data hosting platform for meteorological observations run by the Norwegian Meteorological Institute. This dataset also contains precipitation type observations from sensors other than disdrometers other sensor types, such as the Vaisala PWD12/31 and DRD11A. To ensure a more controlled comparison between sensors, we removed data from non-disdrometer sensors, using a Using a registry provided by the road authorities. we selected time series which was generated using the OTT Parsivel and OTT Parsivel². This was done to ensure a more controlled comparison between sensors. The disdrometers are placed at least 4 meters above the road at automated meteorological stations located along the roads in Norway and provide an estimate of the precipitation type every 10 minutes. The disdrometer precipitation is classified instruments classify precipitation as light rain, rain, snow, and hail. No precipitation, or dry weather, is denoted *dry* in the following. We simplified this the classification by merging the classes light rain and rain since they should appear similar in the CML and radar. Further, as there were few hail events. Additionally, since hail events were rare in the dataset (less than 0.01%) and were not of interest to our study, we set time steps where the disdrometer recorded hail to dry. This adjustment

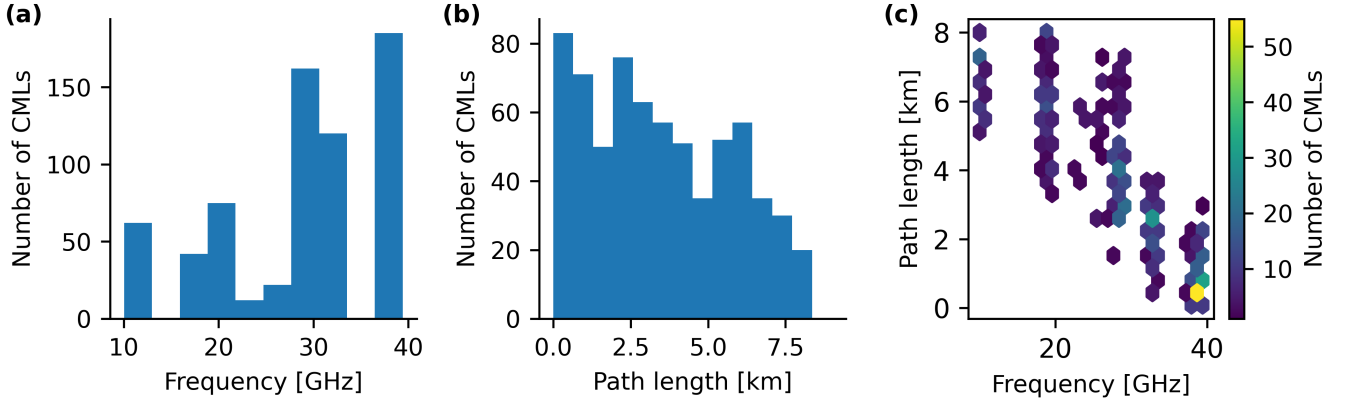


Figure 1. CML characteristics for the summer and winter dataset. (a) Distribution of CML frequencies. (b) Distribution of path lengths. (c) Relationship between path length, frequency, and number of CMLs.

resulted in a negligible error while simplifying the methodology. Thus from the simplifications the disdrometer only records, the disdrometers only report 3 classes: dry, rain and snow. Pairs of CMLs and disdrometers within 8 km of each other were identified using methods from poligrain (2024) and CMLs longer than 8 km were removed. The threshold of 8 km was a trade-off between getting a large number of CML-disdrometer pairs, while still maintaining good correlation between the pairs. This resulted in 550 CMLs and 113 376 CMLs and 83 co-located disdrometers for December 2021 and 435 CMLs and 74 304 CMLs and 60 co-located disdrometers for June 2020. We refer to these as the winter and summer datasets respectively. The CMLs used in the study had signal quantization equal to 0.3 dBm, lengths ranging from 0.4 to 8 km and operated at frequencies between 10 to 40 GHz, with the majority (90 percent) operating above 18 GHz.

(Fig. 1).

2.3.1 Temperature, humidity and dew point temperature

Temperature and humidity data was were downloaded from THREDDS (2024). The data is a downscaled version of ERA5 data on a 1 km grid with a temporal resolution of 1 hour (MET, 2024; Lussana et al., 2021, 2019). It should be noted that model data carries inherent uncertainties due to factors like model assumptions and the data down-scaling, and thus the model data used do not perfectly represent the ground truth. For each CML, we extracted the temperature and humidity at the midpoint of the CML. To account for air humidity we calculated the dew point temperature using the approximated relation with air temperature provided by Lawrence (2005), given as

$$T_d = T_a - ((100 - RH)/5),$$

$$T_d = T_a - ((100 - RH)/5),$$

(1)

where T_d ($^{\circ}\text{C}$) is the dew point temperature, T_a ($^{\circ}\text{C}$) is the air temperature and RH (%) is the relative humidity.

2.4 Classification of ~~rain~~-rainy and ~~snow~~-snowy hours using the ~~radar-temperature~~-disdrometers, the CML-radar (RTCR) method and ~~CML-radar~~-the radar-temperature (CRRT) methodsmethod

The ~~first-method~~-weather radar (5-minute resolution), temperature model (60-minute resolution), CML (1-minute resolution), and disdrometer (10-minute resolution) provide estimates at different locations and with varying time resolutions. This lack of synchronization could potentially lead to erroneous comparisons. To address this issue, we aggregated the precipitation type estimates to hourly intervals to help smooth out these differences.

The "CML-radar" (CR) method uses CML wet periods, as predicted by the wet-dry estimation method, to classify precipitation as rain. Next, since the CMLs are not noticeably attenuated by dry snow, radar precipitation without corresponding CML precipitation is classified as snow. To aggregate the CR estimates to hourly resolution, we classified hours as rainy if the CML rainfall classification algorithm recorded any rainfall, snowy if the radar estimated any precipitation but the CML did not estimate rainfall, and dry otherwise. The "radar-temperature" (RT) ~~-method~~ uses surface temperature and weather radar to determine precipitation occurrence and precipitation type. As recommended by Harder and Pomeroy (2014), humidity is accounted for by using the dew point temperature. The RT method then works by ~~classifying radar~~-estimating the average precipitation along the CML, and classifying precipitation above a dew point temperature threshold as rain and below the threshold as snow. ~~In line with Marks et al. (2013) the~~ The dew point temperature ~~threshold is~~-was evaluated at the pixel closest to the center of the CML and was, in line with Marks et al. (2013), set to 0°C . Combining humidity-corrected temperature models with weather radar is a common method and is often used as a reference method (Casellas et al., 2021; Saltikoff et al., 2015; Gjertsen and Ødegaard, 2005). ~~The second method, "CML-radar" (CR), uses the CML wet periods as an indicator for whether it is raining or not. Since the CML is not noticeably attenuated by dry snow we can set radar precipitation that is not accompanied by CML precipitation as snow. The CR method predictions is summarized in Table ??.~~ To aggregate the RT estimates to hourly resolution we classified hours as dry if the radar observed no precipitation. If the radar observed precipitation, we classified the hours as rainy or snowy based on whether the dew point temperature was above or below 0°C , respectively. For the disdrometers, we classified hours as rainy if the disdrometer recorded any rain during that hour, snowy if the disdrometer recorded snow but no rain, and dry otherwise.

The drawback of the aggregation method is that we overestimate the number of rainfall events, introducing more uncertainties in the results. However, we consider this an acceptable trade-off as it allows for a more consistent analysis. The effects of the aggregation method are evaluated further in the discussion.

2.5 Metrics

In this study we will consider both binary classification (for instance, rain and not-rain) and multiclass classification (rain, snow and dry). A common tool for visualizing the performance of a classification algorithm is to use a confusion matrix. It compares the ground truth labels with the predicted labels, allowing us to understand the types of errors made by the classifier.

Table 1. ~~Radar and CML~~ Confusion matrix for binary classification. The positive class typically represents snow, rain, or both, while the negative class represents all other conditions ~~and not included in the CR method predictions~~ positive class.

	Radar-rain Predicted: Negative	Radar-dry Predicted: Positive
CML-rain Ground truth: Negative	Rain True Negative (TN)	Rain False Positive (FP)
CML-dry Ground truth: Positive	Snow False Negative (FN)	Dry True Positive (TP)

In this study the classifier is either the CR or RT method and the ground truth is the disdrometers. In the binary case, the labels are categorized as either negative or positive (Table 1).

210 2.6 Performance metrics

~~We~~ Using this confusion matrix, several metrics can be defined. We will first consider the the accuracy score, which relates the proportion of true results by the total number of cases examined such that

$$\text{Accuracy} = \frac{\text{TN} + \text{TP}}{\text{TN} + \text{TP} + \text{FP} + \text{FN}}. \quad (2)$$

215 Because of its simplicity, accuracy is a widely used metric, but it may not always be the best indicator of classifiers performance, especially in cases of imbalanced datasets. To better understand the performance of the classifiers it is therefore common to consider other metrics as well. The precision score focuses on the classifiers positive predictions and provides the ratio between the false and true positive predictions, such that

$$\text{Precision} = \frac{\text{TP}}{\text{TP} + \text{FP}}. \quad (3)$$

It is also common to consider the recall score, which gives the proportion of reference positive cases predicted by the classifier

220

$$\text{Recall} = \frac{\text{TP}}{\text{TP} + \text{FN}}. \quad (4)$$

Since any classifier typically must strike a balance between false positives and false negatives, improving the precision comes at the expense of the recall. To consider both recall and precision, the F1 score estimates the harmonic mean of the precision and recall, combining these two metrics such that

$$225 \text{ F1} = 2 \times \frac{\text{Precision} \times \text{Recall}}{\text{Precision} + \text{Recall}} = \frac{2\text{TP}}{2\text{TP} + \text{FN} + \text{FP}}. \quad (5)$$

We also use the Matthews correlation coefficient (MCC) to quantify the performance of the classification methods. The MCC is a ~~statistical measure that provides a balanced evaluation metric, yielding~~ metric that has been shown to outperform the accuracy and F1 score on imbalanced datasets, by indicating a good correlation only when the classifier performs good on both positive

and negative cases (Chicco and Jurman, 2020). The MCC is given by

$$230 \quad \text{MCC} = \frac{\text{TP} \cdot \text{TN} - \text{FP} \cdot \text{FN}}{\sqrt{(\text{TP} + \text{FP}) \cdot (\text{TP} + \text{FN}) \cdot (\text{TN} + \text{FP}) \cdot (\text{TN} + \text{FN})}}. \quad (6)$$

The accuracy, precision, recall and F1 score reach their best value at 1 for a perfect estimate and worst score at 0. The MCC score of 1 indicates a perfect prediction, 0 if the estimate are no better than random guesses, indicates a random guess and -1 for complete disagreement between estimate and observation (Chicco and Jurman, 2020) is a perfect inverse prediction.

In the multiclass case, the hourly predicted estimates compared to the hourly ground truth can be summarized in a multiclass confusion matrix, see Table 2. The accuracy score can be extended to the multiclass case as follows

Table 2. Multiclass confusion matrix of the ground truth (disdrometer) and predictions (CR and RT method).

	<u>Predicted: Dry</u>	<u>Predicted: Rain</u>	<u>Predicted: Snow</u>
<u>Ground truth: Dry</u>	<u>True Dry</u>	<u>False Rain</u>	<u>False Snow</u>
<u>Ground truth: Rain</u>	<u>False Dry</u>	<u>True Rain</u>	<u>False Snow</u>
<u>Ground truth: Snow</u>	<u>False Dry</u>	<u>False Rain</u>	<u>True Snow</u>

235

$$\text{Accuracy} = \frac{\text{True dry} + \text{True rain} + \text{True snow}}{\text{Total number of instances}}. \quad (7)$$

The precision, recall and F1 scores are slightly more complicated to generalize, as they involve selecting specific parts of the binary confusion matrix. In this study, we evaluated 3 classes, work we generalized the precision, recall and F1 scores using macro averaging, which works by evaluating each class (dry, rain and snow, making this a multiclass problem. For evaluating the classification of rainfall alone (MCC_{rain}), we considered two classes, rain or no rain. Thus for MCC_{rain}, dry and snow are in the same category. Likewise for snow (MCC_{snow}), dry and rain are in the same category. For the combined classes (MCC_{all}) we compute the multiclass MCC for all three categories, dry, rain and snow. The MCC_{all}, MCC_{rain} and MCC_{snow} snow) individually and then averaging them into a single number.

245 Following Gorodkin (2004), the MCC metric can be generalized to n classes, providing a balanced metric that uses the full confusion matrix (Jurman et al., 2012). The MCC between the reference x and the predictions y for the multiclass case is given by

$$\text{MCC} = \frac{\text{cov}(X, Y)}{\sqrt{\text{cov}(X, X) \cdot \text{cov}(Y, Y)}}, \quad (8)$$

where

$$\text{cov}(X, Y) = \frac{1}{N} \sum_{k=1}^N \text{cov}(X_k, Y_k), \quad (9)$$

250 where N is the number of classes and $\text{cov}(X_k, Y_k)$ is the covariance between the reference X_k and the predictions Y_k for class k . All metrics were computed using *scikit-learn* (Pedregosa et al., 2011) ~~which in the multiclass case implements MCC based on Gorodkin (2004).~~

3 Results

3.1 Practical application investigating road friction ~~Case study~~

255 As a practical application, we studied how road friction, as measured at a meteorological station operated by the Norwegian road authorities, was related to the predictions from CR and RT methods. The meteorological station is located at Hålogalandsbrua bridge close to Narvik and the CML is located within 5 km distance. To illustrate the RT and CR method, we first focus on a case study performed over a large area in mid-Norway, covering 36 CML-disdrometer pairs over a two day period from the 18th to the meteorological station. We studied 11 days of data where the meteorological station recorded a broad range
260 of weather events. The data from the road authorities included road condition as measured by a Vaisala remote surface state sensor DSC211, precipitation type as measured by a OTT Parsivel², the road temperature as measured by a Vaisala remote road surface temperature sensor DST111 and road friction as measured by a Vaisala remote surface state sensor DSC211. Road friction is rated from 20th of December 2021 (Fig. 2). The area spans from the Trondheim fjord and Norwegian coast in the north and west, to the Dovre mountain in the south. For each CML we counted the number of snowy and rainy hours estimated
265 by the RT method (a, d), CR method (b, e) and the nearby disdrometer (c, f). The total snowy and rainy hours were then interpolated using inverse distance weighting, with the midpoint of the CML indicating its position. We can observe that at the location of CML1 and CML2 (mountainous areas) the RT and CR method estimates more snow and less rain compared to the disdrometers. At the location of CML3 the RT method estimates more snow and less rain compared to the CR method and disdrometers.

270 Examining the time series for CML1 and CML2 (Fig. 3 and Fig. 4), we observe that before 18:00 on December 18th, the dew point temperature (b) is mostly above 0 degrees, and the CML signal level fluctuates markedly (c), especially during periods when the weather radar estimates rainfall. After 18:00, as the temperature drops well below 0 degrees, the CML signal loss shows a different pattern with much less fluctuation. Around 18:00, the CR method, RT method, and disdrometer all estimate rainfall. After 18:00, the CR and RT methods estimate snow, while the disdrometer shifts between rain and snow. Before 18:00,
275 the RT method estimates some rainfall while the CR method estimates snow, possibly because the rainfall event was not strong enough for the CML wet detection algorithm to identify it as rainfall.

The time series for CML3 indicates a different climatological pattern compared to CML1 and CML2, with temperatures above zero before 18:00 on December 18th and hovering around zero degrees afterward (Fig. 5). Observing the CML time series, we see that the signal loss fluctuates during all time steps when the radar estimates precipitation. The disdrometer
280 primarily indicates rainfall, except for a period from 00:00 to 1, typically at 0.82 for dry roads, 0.7 for wet roads, and between 0.4-0.9 on December 19th, when it shows a mixture of rain and snow. In contrast, the RT method indicates a longer snowy period, lasting from 19:00 on the 18th to 0.6 for snowy or icy roads. No pre-processing of these data was performed. 14:00 on

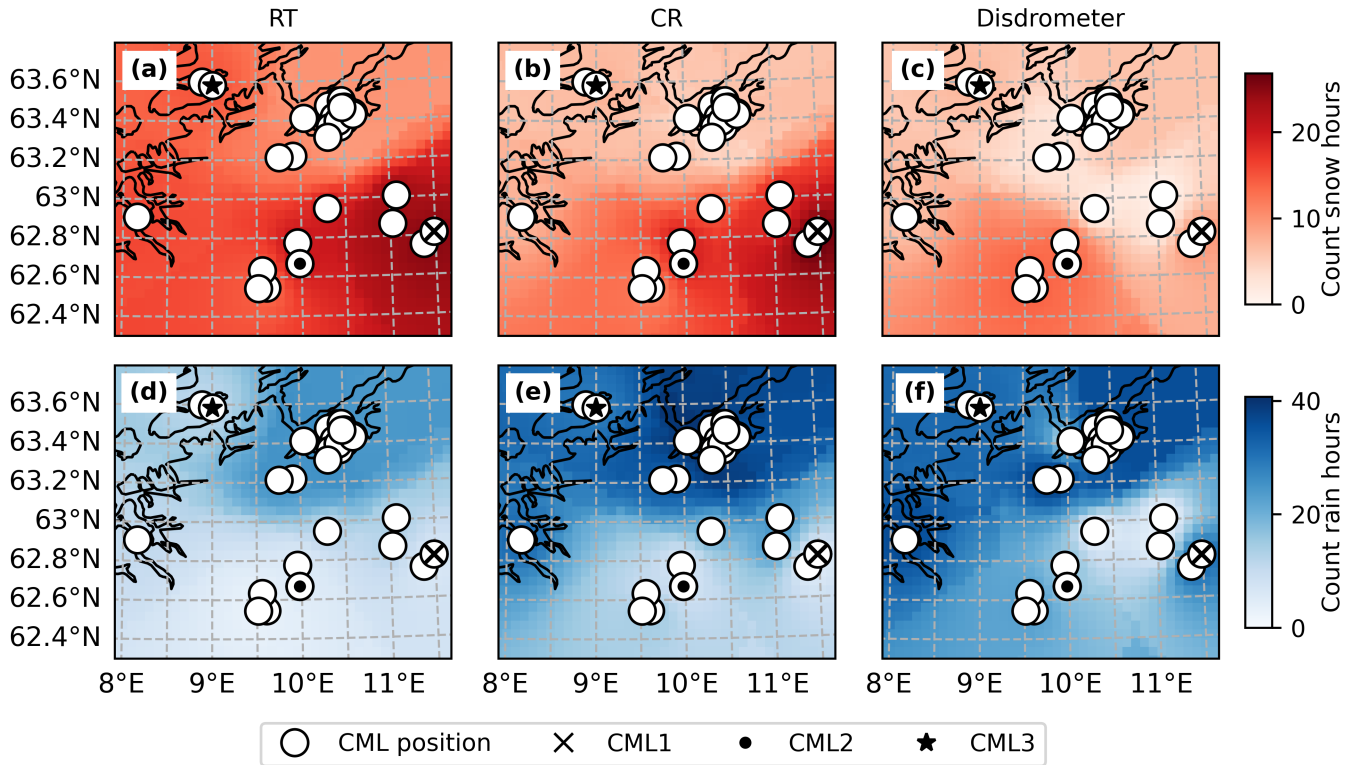


Figure 2. Interpolated count of rainy (a, b, e) and snowy (d, e, f) hours for the RT method (a, d), CR method (b, e) and disdrometers (c, f) over a 2-day period starting on the 18th of December 2021. The Trondheim fjord and Norwegian coast (black line) are in the north and west, while the Dovre mountains are in the south. White circles indicate the (distorted) positions of the CMLs. The black x, dot, and star represent the locations of CML1, CML2, and CML3, respectively, with their time series shown in Fig. 3, Fig. 4, and Fig. 5. The maps were interpolated using inverse distance weighting, with the midpoint of the CML indicating its position.

the 19th. The CR method primarily estimates rainfall but identifies short snowy periods around the disdrometers snow period, and estimates rainfall when the disdrometer indicates snow.

285 4 Results

3.1 Overview of the data as a function of dew point temperature

Our dataset consists of CML-disdrometer pairs from the summer dataset and the winter dataset. Every minute each pair provides several different observations such as disdrometer-observed precipitation type, dew point temperature and CML signal loss. In Fig. ?? we have plotted histograms of the number of minutes (first row), the observed disdrometer precipitation type (second row) and CML and radar precipitation (third row) for To get an overview of the full dataset used in the study, we counted the total number of rainy and snowy hours estimated by the disdrometers, RT method, and CR method for 1-degree dew point

290

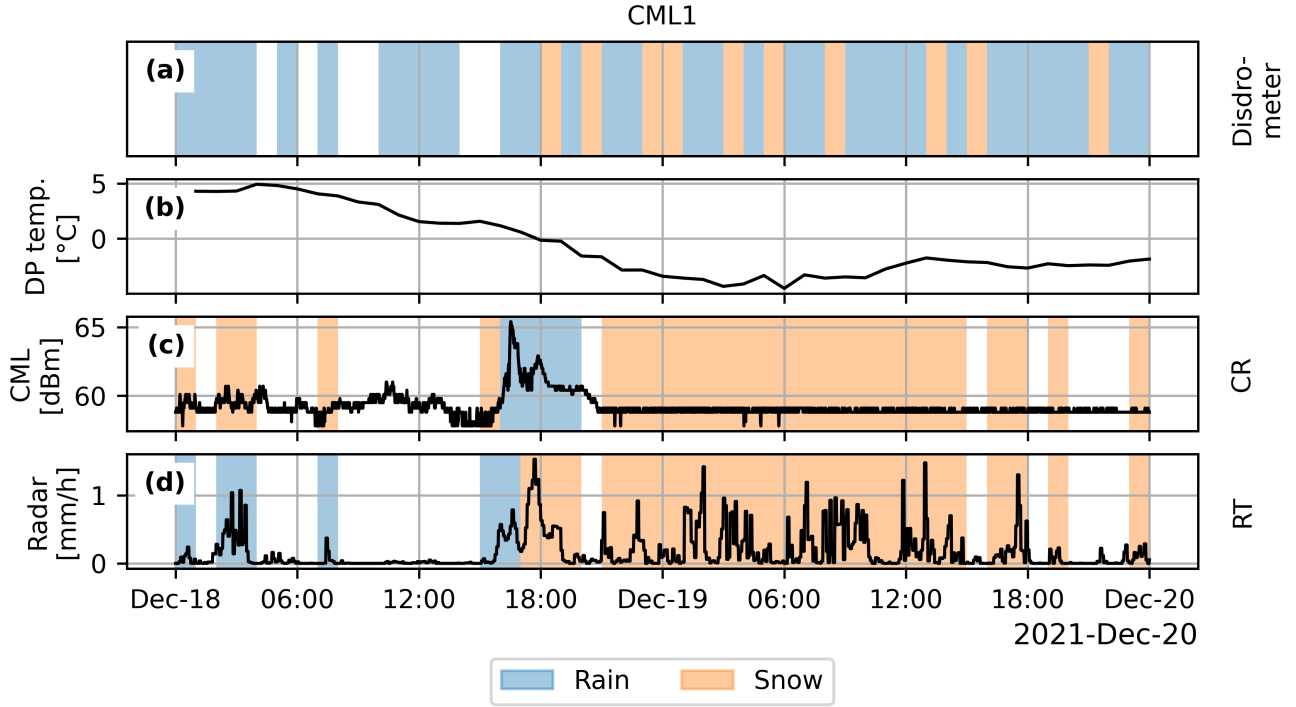


Figure 3. Time series for CML1 located in the eastern mountain area of Fig. 2. Dew point temperature (b), CML signal loss (c), and radar rainfall (d). Shaded areas indicate the precipitation type (rain or snow) estimated by the disdrometer (a), the CR method (c), and the RT method (d).

temperature intervals of 1-degree between -20 and 20 degrees. From the disdrometer observations we can observe that all of our data is between -20 and 20 degrees with most of the (Fig. 6). Our data covers the full temperature range, with most observations concentrated between -10 and 10 degrees. The disdrometers record snow mainly below zero degrees with some recorded (a), with some snow events slightly above zero degrees. For disdrometer rainfall, most rainfall is. Most rainy hours recorded by the disdrometers occur above zero degrees, but there is-are also a substantial amount of rainfall recorded below. The CML also detects wet precipitation number of rainy hours recorded below zero. The CR method also estimates rainy hours below zero degrees, but not as frequently as the disdrometers. The weather radar detects more wet minutes around 10 degrees compared to the CML but it records fewer snowy minutes around -10 degrees compared to the disdrometer. We can also observe that the weather radar detects fewer events below -10 degrees as compared to the disdrometer. Frequency (counts of minutes) as a function of dew point temperature (T_d) for number of recordings (first row), disdrometer recorded rain and snow (second row) and CML recorded rain and radar recorded precipitation (third row).

3.2 The performance of the CR method vs. the RT method

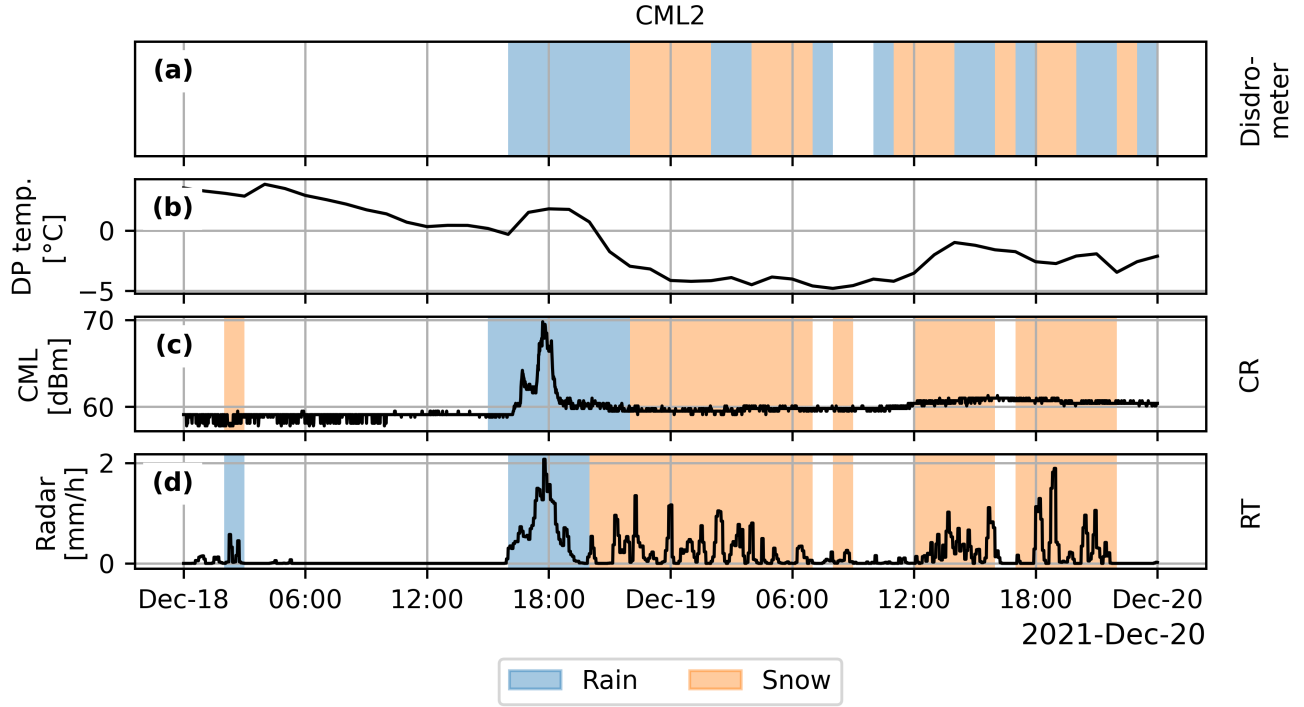


Figure 4. Time series for CML2 located in the southern mountain area of Fig. 2. Dew point temperature (b), CML signal loss (c), and radar rainfall (d). Shaded areas in indicate the precipitation type (rain or snow) estimated by the disdrometer (a), the CR method (c), and the RT method (d).

The performance of the RT and CR methods is visualized in scatter density plots using monthly time series for each CML-disdrometer pairs (Fig. 8). We can observe that for MCC_snow both methods perform quite similarly, while for MCC_rain CR seems to perform on average better than RT. For the combined classification the MCC_all is similar for both high RT and high CR scores, while for lower RT scores CR performs better. Looking at the mean dew point temperature we can observe that for MCC_all and MCC_rain there is a gray cluster above the black line, indicating that the CR method in general improves the estimates for CMLs with a monthly mean temperature around zero degrees. Moreover, rainfall classification has a poorer score at lower average temperatures and snow classification has a poorer score at higher temperatures. First row: Scatter density plots comparing the MCC_all, MCC_rain and MCC_snow of the CML-based classification method CR and the reference method RT using the disdrometers as reference. The MCCs are computed for each CML-disdrometer pairs using 1 month of data. Second row: Same scatter density plots, but the cells show the mean dew point temperature (T_d) of each cell.

The MCC for all classes (MCC_all), for the rainfall class only (MCC_rain) and for the snow class only (MCC_snow) is plotted as a function of dew point temperature between -10 though less frequently than the disdrometers, and it estimates a significant number of snowy hours above zero degrees (c). The RT method, by definition, predicts rainy hours above zero degrees and 10 degrees (Fig. ??). We can observe that for the multiclass MCC_all both the CR and RT methods perform similar

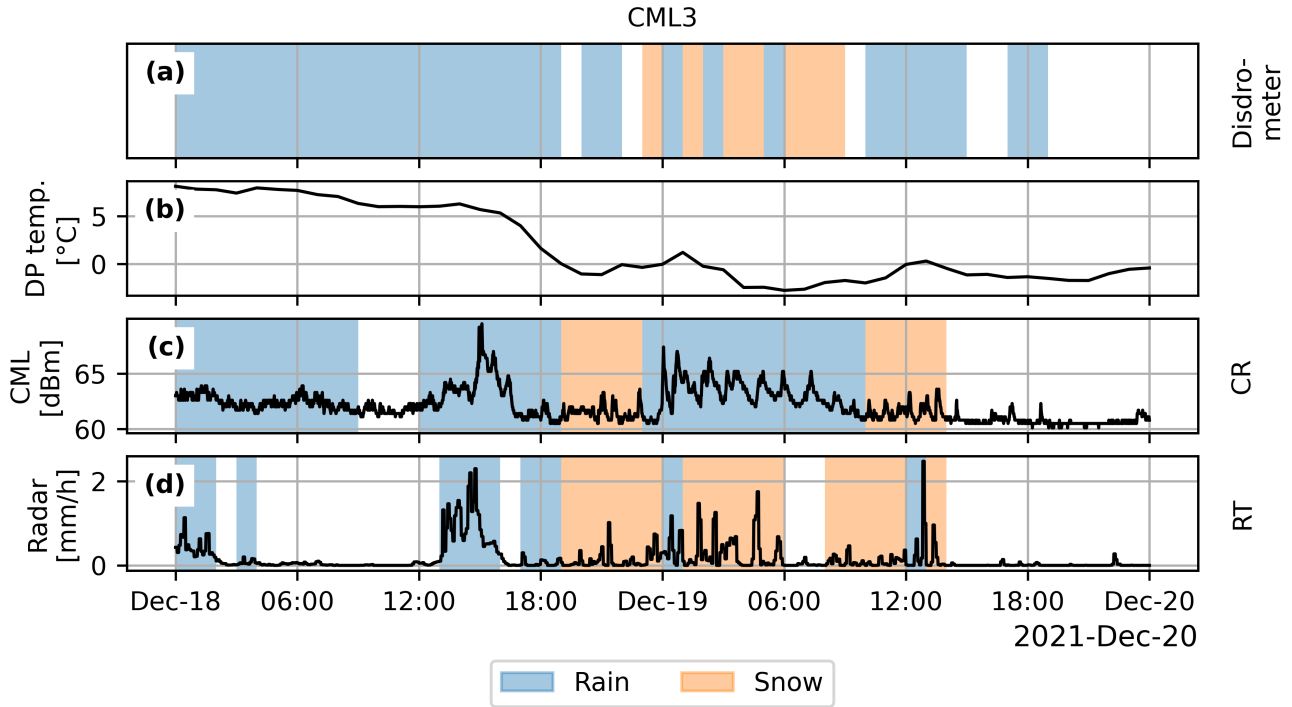


Figure 5. Time series for CML3 located in the north western coastal area of Fig. 2. Dew point temperature (b), CML signal loss (c), and radar rainfall (d). Shaded areas in indicate the precipitation type (rain or snow) estimated by the disdrometer (a), the CR method (c), and the RT method (d).

for low dew point temperature and high dew point temperature, while snowy hours below zero degrees (b). Additionally, we observe that the RT method estimates fewer rainy hours than the CR method is superior in the dew point temperature range -1 to -7, even above zero degrees.

3.2 Precipitation bias as a function of temperature

The difference between the estimated CML rainfall amounts and the ground truth radar rainfall amounts is plotted as a function of dew point temperature (Fig. ??). The CML rainfall amounts were computed by using the weather radar wet period (left column) and by using the CML wet period (right column). 7 (a). For dew point temperatures below -2 degrees, we observe that there is a positive bias where the radar in general overestimates the precipitation amounts compared to the CML. For dew point temperature around zero generally estimates more precipitation. Between 0 and 2.5 degrees, there seem to be many more events where there is a negative bias, meaning that the CML overestimates the rainfall amounts compared to the radar is a stronger negative bias where the CML estimates more precipitation. For dew point temperatures above 4 degrees, the CML and radar estimate has estimates show a similar spread. When using the CML to identify wet and dry periods, we more often observe a large negative bias compared to when the radar is used to identify wet and dry periods. In

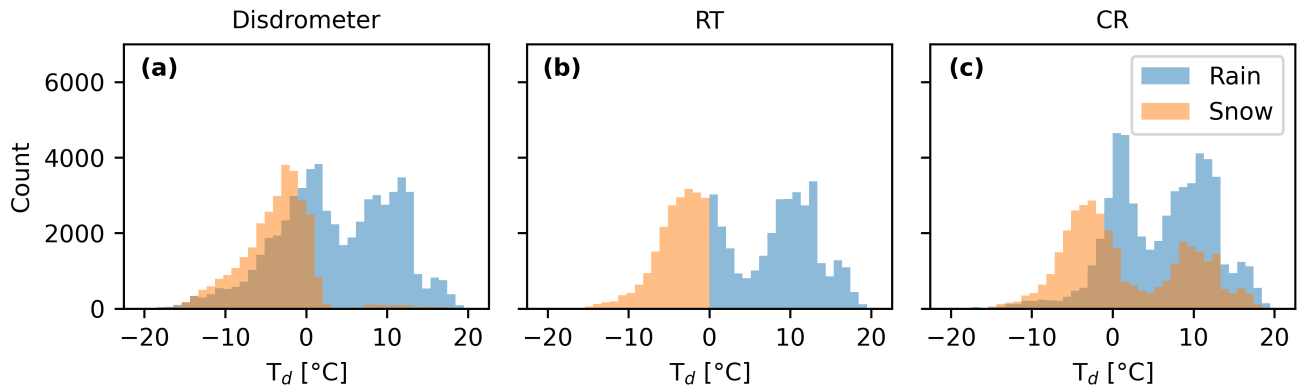


Figure 6. Matthews correlation coefficient for snow and rain (MCC_all), for rain (MCC_rain) and snow (MCC_snow) as a function Number of hours classified as snowy or rainy for dew point temperature (T_d) intervals of 1 degree ranging between -20 to 20 degrees for the disdrometers (a), RT (b) and CR (c) estimates.

the second, third and fourth row, we have plotted the fraction of hours within the bins where the disdrometer recorded at least 10 minutes of rain, snow and both snow and rain (mix) respectively. We observe that there is a lot of rain. In panels (b) and (c) the color of the cell indicate the proportion of rainy or snowy hours over total hours for each cell in panel (a). Generally, there is more rainfall in observations above zero degrees, while there is a lot of -2.5 degrees and more snow in observations below zero degrees. Around zero degrees, we have observations of both rain and snow, and some hours where both rain and snow have been observed. We can also observe that for rainfall there is a larger proportion of the cells that experience more than 10 minutes of rainfall for negatively biased events, -2.5 degrees. Additionally, for events where the CML estimates more rainfall compared to the radar (negative bias), there are more rainy hours as observed by the disdrometer.

3.2 Map The performance of the CR and method vs. the RT precipitation estimates method

Fig. 2 displays a map showing the precipitation type estimated at the CML locations using the RT method (left column), the CR method (middle column) and The performance of each CML-disdrometer pair for the RT and CR methods is compared on the summer and winter dataset using scatter density plots (Fig. 8, (a, b, c, d, e)). In the lower row (f, g, h, i, j), the disdrometer observations (right column) for 1-hour accumulation periods. The RT method estimates rain (CML-rain) if the weather radar observed rainfall for more than 5 minutes while the dew point temperature was positive, snow if the weather radar observes precipitation for more than 5 minutes while the mean dew point temperature was negative (CML-snow), mix if both rain and snow was recorded for more than 5 minutes (CML-mix) and no precipitation otherwise (CML-dry). The CR method estimates rain when the CML recorded more than 5 minutes of rainfall (CML-wet), snow when the radar recorded rainfall while the CML did not for more than 5 minutes (CML-snow), mix if both rain and snow was recorded for more than 5 minutes (CML-mix) and dry otherwise (CML-dry). The disdrometers estimate rain when more than 10 minutes of rain is recorded (Dsd-rain), snow

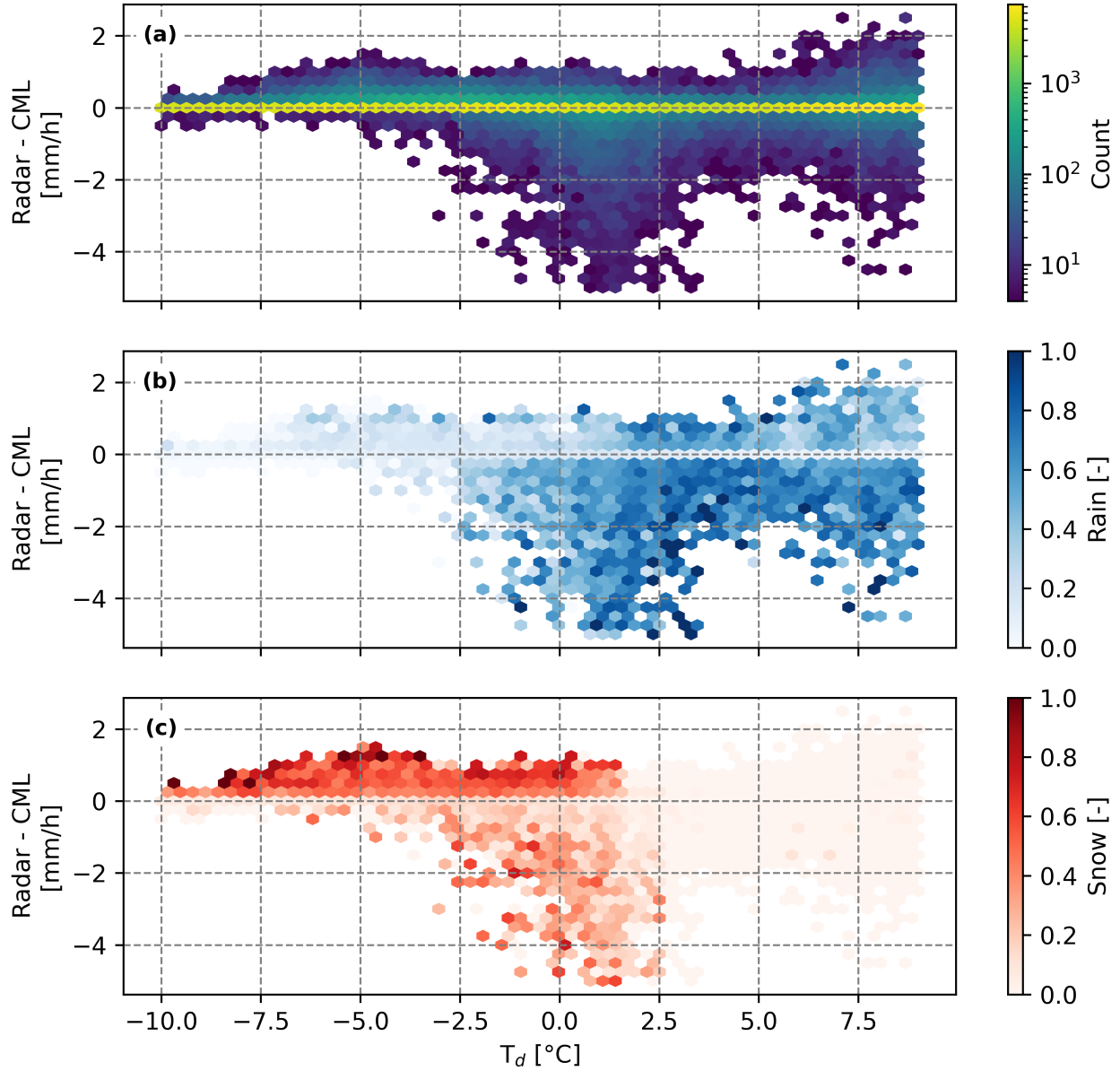


Figure 7. First row: (a): Difference between hourly precipitation amounts as measured by the radar and CML as a function of dew point temperature (T_d). CML rain amounts were estimated using wet periods identified by the weather radar (left column) and the CML (right column). Second, third, and fourth row: The fraction intervals of the hours within the bins where the disdrometer recorded at least 1 degree ranging between -10 to 10 minutes degrees. (b, c): Ratio of rainfall, snow, rain and both snow and rain (mixed precipitation), respectively in each cell as observed by the disdrometer. Cells with less than 4 events are not shown.

350 when more than 10 minutes of snow is recorded (Dsd. snow), mix when both rain and snow are recorded (Dsd. mix), and dry conditions otherwise (Dsd. dry).

Overall we can observe that in the south part of each CML disdrometer pair is shown. Note that some cells consist of several CML-disdrometer pairs and that the map indicated temperature then is the average of all pairs in the cell. In terms of accuracy (a, f), both the CR and RT method gives similar estimates, while in the middle and north the CR and RT method estimate a mixture of rain and snow. Looking at the CMLs located around point A (black cross) we can observe that in the first three time steps the RT method estimates more rainfall while methods perform similarly well, with a few CMLs performing less well using the CR method. For precision (b, g), we observe that, on average, the RT method outperforms the CR method estimates more mixed precipitation and the disdrometers observe mixed precipitation. In the forth time step both RT and CR estimates rain, snow and mix, while, indicating that the RT methods positive predictions are more trustworthy than those of the CR method. However, the CMLs where the CR method performs less well tend to have an average temperature above 5 degrees, while for colder temperatures, the RT and CR precision scores are more similar. In terms of recall (c, h), the CR method performs slightly better than the disdrometers observe snow and mix. In the last time step the RT method estimates rainfall, indicating that the CR method estimates more snow and the disdrometers observes mostly snow.

A 50 x 100km area in Norway observed in 1-hour intervals from 00:00 to 04:00 on 19th December 2021. The left column show CML condition using the RT method, the middle column show the CML condition using the CR method and the right column show the disdrometer observations. The colors reflect the estimated weather conditions dry (black), rainy (blue), snowy (cyan) and dry (red). The black x indicates point A for orientation. Coordinates are not shown due to data security reasons.

3.3 Precipitation type and road friction

In a practical application of our study, we analyzed CML data and weather radar data at the CML location. This data was then compared with observations from a meteorological station in Narvik (Fig. ??). is better at correctly identifying the disdrometer precipitation type. Looking at the CML time series (TL), we observe that around the 12th, the CML does not indicate any rainfall, while the radar observes precipitation and the disdrometer observes snow. Simultaneously, the road condition indicates snow and road friction drops rapidly. This suggests that the observed precipitation consists of dry snow, which is likely responsible for the reduction in road friction. Moving to the next event, we can F1 score (d, i), which combines the precision and recall score, we observe that the road friction drops again between the 13th and 14th, but there is no recorded precipitation from either the radar or the disdrometers. From the road condition, we can observe that the road has transitioned from damp to ice, indicating that the road friction is low due to water that has frozen. Next, between the 15th and 16th, there is a drop in the road friction where the disdrometers and road condition indicate snow. However, the CML indicates a wet period. Comparing the difference between the CML and weather radar we see that the CML overestimates rainfall by more than CR method performs worse on average when the temperature is above 5 mm for those hours. Looking at the TL of the CML we observe that the TL has a more gradual increase, not like the more variable pattern seen at the next time steps where the disdrometer and road condition indicate that it is raining. Given that the disdrometers indicate snow and the CML indicates a wet period, this could suggest that the decreased road friction is caused by wet snow. Interestingly, this event caused a larger

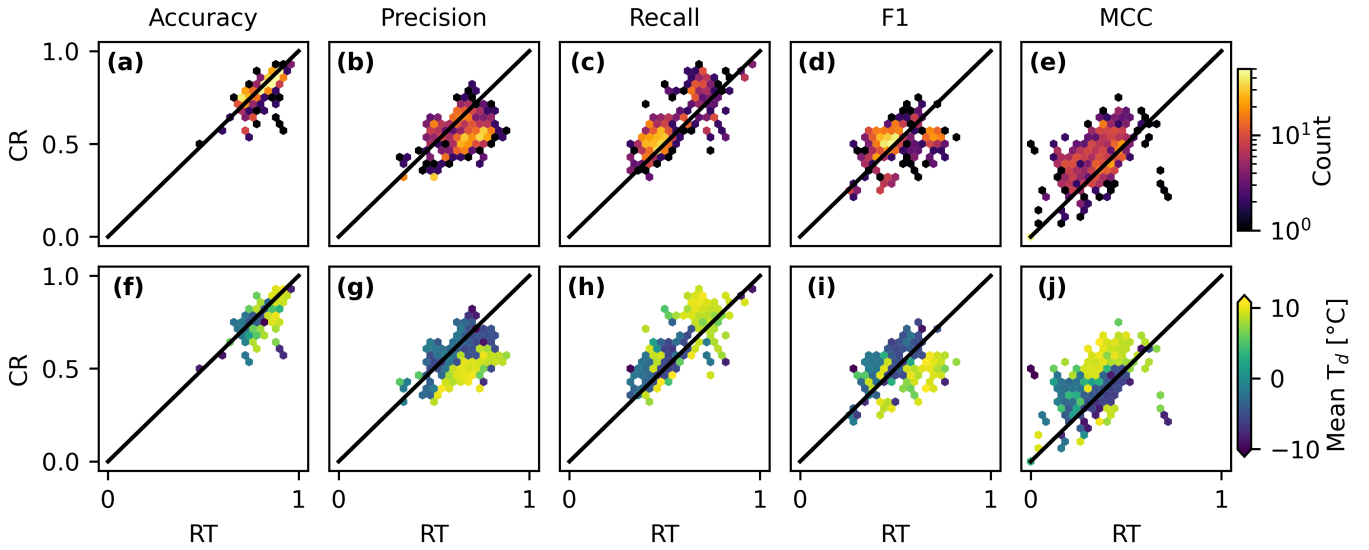


Figure 8. Scatter density plots (a, b, c, d, e) comparing the accuracy, precision, recall, F1 and MCC score for the CR and RT method for each CML-disdrometer pairs. Average dew point temperature of each cell (f, g, h, i, j).

drop in road friction than the two previous events on the 12th and 14th. After this event, the disdrometer and road condition indicate a long rainy period between the 16th and 19th. This is supported by the CML and radar estimating approximately the same amounts of rainfall. Just before the 19th, there is a short period where the CML overestimates rainfall amounts and the disdrometer records snow. However, the period is so short that the road friction is not dropping. Finally, between the 19th and 20th, there is a large drop in road friction where the CML also overestimates rainfall amounts compared to the radar, and the disdrometer records snow. This could again indicate that the decreased road friction is caused by wet snow.

Fig. ?? also shows that during the rainy period between the 16th and 19th, the CR method estimates switches more between degrees, but better when the temperature is below 5 degrees. Lastly, looking at the MCC score (e, j), the CR method outperforms the RT method for most CML-disdrometer pairs.

To investigate the effect of temperature on the CR and RT predictions we plotted the multi-label confusion matrix of the two methods for the three temperature intervals -20°C to -2°C (a, d), -2°C to 2°C (b, e) and 2°C to 20°C (c, f) (Fig. 9). The corresponding accuracy, precision, recall, F1 and MCC scores for the individual classes (rain and snow) as well as the multiclass score are shown in Table 3. We can observe that, compared to the RT method, the CR method generally identifies more correct rainfall events. It also identifies more snowfall events in the temperature interval -2 to 2 degrees.

4 Discussion

4.1 Evaluation of the disdrometers performance

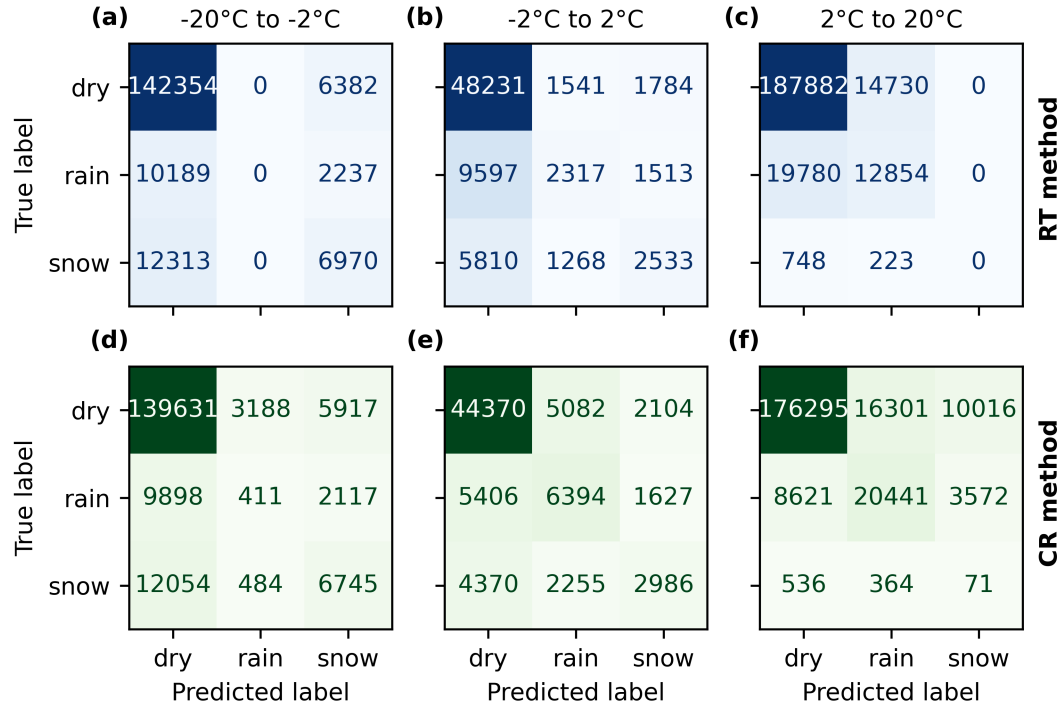


Figure 9. Confusion matrices for the RT (a, b, c) and CR (d, e, f) method for three temperature intervals.

Table 3. Accuracy, precision, recall, F1 and MCC score for the RT and CR method for different temperature intervals. The "Rain", "Snow" and "Multi" columns indicates whether the metric was evaluated against rainfall only, snow only or if it used the generalized multiclass metric to evaluate both rain and snow.

	-20°C to -2°C			-2°C to 2°C			2°C to 20°C			All temperatures		
	Rain	Snow	Multi	Rain	Snow	Multi	Rain	Snow	Multi	Rain	Snow	Multi
Accuracy RT	0.93	0.88	0.83	0.81	0.86	0.71	0.85	1.00	0.85	0.88	0.93	0.82
Accuracy CR	0.91	0.89	0.81	0.81	0.86	0.72	0.88	0.94	0.83	0.88	0.91	0.81
Precision RT	0.93	0.69	0.66	0.65	0.67	0.55	0.68	1.00	0.68	0.68	0.70	0.59
Precision CR	0.52	0.69	0.47	0.68	0.67	0.58	0.74	0.50	0.50	0.71	0.62	0.56
Recall RT	0.50	0.65	0.44	0.56	0.61	0.46	0.66	0.50	0.44	0.61	0.65	0.51
Recall CR	0.51	0.65	0.44	0.68	0.63	0.55	0.77	0.51	0.52	0.70	0.64	0.56
F1 RT	0.48	0.67	0.44	0.57	0.63	0.47	0.67	0.50	0.45	0.63	0.67	0.53
F1 CR	0.50	0.67	0.45	0.68	0.64	0.56	0.76	0.49	0.50	0.71	0.63	0.56
MCC RT	0.00	0.34	0.30	0.19	0.27	0.28	0.34	0.00	0.34	0.28	0.34	0.32
MCC CR	0.02	0.34	0.27	0.35	0.30	0.39	0.52	0.00	0.47	0.41	0.25	0.39

400 The disdrometer data suggest that rain is more frequent below zero degrees than snow is above zero degrees (Fig. 6), which could indicate that the disdrometer overestimates the number of rainy hours. For example, looking at the CML time series (Fig. 3), the disdrometer shows a mix of rain and snow compared to the RT method. This, while the CR and RT methods indicate only snow. This discrepancy could be due to that there is a mixture of snow and rain at temperatures close to zero degrees. It could also be that the CML and weather radar are not perfectly synchronized, causing the CR method to predict snow for instance when the weather radar detects rainfall shortly before the CML. Time series for the meteorological station in Narvik operated by the Norwegian road authorities. The first row shows the road condition dry (white), damp (light blue), wet (green), slush (orange), snow (purple) and ice (brown). The next row shows whether the disdrometer records no (white), liquid (blue) or solid (orange) precipitation. The third row shows the dew point temperature (orange) and the temperature measured by a sensor mounted next to the road (blue). The fourth row shows the road friction as measured by a sensor in the road. The fifth row shows the total loss of a nearby CML (TL) as well as the estimated wet (blue) and snowy (red) periods using the CR method. The sixth row shows the radar precipitation amounts (blue line) measured as a weighted sum along the CML as well as snowy (red-shade) and rainy (blue-shade) periods as estimated by the RT method. The seventh row shows the difference between the radar and CML rainfall amounts (blue line) as well as the time steps where the difference is less than -5 (blue shade).

5 Discussion

415 4.1 The distribution of rain and snow around zero degrees

The disdrometer data suggest that there is more frequent rainfall the spatial distance between disdrometers and CMLs, with temperature differences at these locations possibly causing rain to be recorded at colder temperatures. However, if this effect were significant, we would also expect to see more snow recorded at temperatures above zero degrees, which we do not observe. Another explanation for these discrepancies could be the aggregation method, where rainy hours are given priority over snowy hours, creating the impression that there are more rainy hours below zero degrees than there is snow above zero degrees (Fig. ??). Although there is no reason to expect that the distribution of rain and snow around zero degrees should be symmetric, observing significant rainfall amounts far below zero degrees is not expected. Comparing the CML wet. However, if the disdrometer was correct and 10 minutes of an hour were indeed rainy, that would still represent a significant amount of rain during that hour. Moreover, comparing the CR rain distribution with the disdrometer rain distribution (Fig. 6), we can see that the CML observes fewer wet events CR method observes fewer rainy hours below zero degrees. We have also observed that snow events around zero degrees can show up as wet in the CML (Fig. ??). Thus, contrary to what we observe, below zero degrees we should expect that the CML estimates more wet events than the disdrometer observes rainfall. This could indicate that the, indicating that the disdrometers overestimate the number of rainy events hours below zero degrees. One reason One explanation for this overestimation could be due to the spatial distance between the disdrometer and that wet snow makes the disdrometer alternate between snow and rain, creating the impression that there is more rain below zero degrees. Moreover, different precipitation type sensors are also known to disagree during mixed precipitation events (Bloemink, 2005; Pickering et al., 2021), indicating that these events are hard to classify. However, while wet snow could explain some of the rainfall events below zero

degrees, the CML midpoint where the temperature is recorded. Since the temperature can be different at those locations due to for instance differences in elevation, we should expect that some rain events are assigned to colder temperatures while others are assigned to warmer temperatures. On the other hand, if this effect played a large role we should also see the same effect for snow, with more snow being recorded up to -10°C. Large proportion of rainy hours below -10 degrees remains puzzling, as wet snow is not expected at such low temperatures. Another explanation could be that wet snow makes the disdrometer alternate between snow and rain, with a stronger emphasis in rain, creating the impression that there is more rain below zero degrees. Other explanations could be errors in the disdrometer classification algorithm or it could come from misclassification by the disdrometer due to factors such as strong winds, particles falling through the edges of the sampling area and splashing. Although correction algorithms exist (Friedrich et al., 2013), they typically require the full velocity-drop size distribution matrix, which our disdrometers do not provide. This limitation may lead to less accurate classifications. Additionally, cars spraying water droplets from salted roads could contribute to the high number of rainfall events recorded below zero degrees. Consequently, while the disdrometer disdrometers provides valuable estimates, it may they do not perfectly represent the ground truth, especially during mixed precipitation events.

4.1 CML dry periods can be used in combination with weather radar to classify dry snow The case study

Below -1 degrees the CR method is able to classify snow with a similar accuracy as the RT method. For temperatures above -1 degrees both the CR and RT method performance decreases, but the CR performance decreases slower than the RT method, indicating The case study indicated that the CR and RT methods estimated a similar number of snow events in the mountains, while along the coast (for instance at CML3), the CR estimates were more in line with the disdrometer estimates, suggesting an advantage of using the CR method for classifying snow in certain climatic zones. This could be due to the warmer conditions along the coast, which keep the temperature around zero degrees, a range where the RT method has more uncertainties. However, looking at the time series of CML3 (Fig. ??). Part of the performance decrease of the CR method could be due to that at higher temperatures the spatial differences between the CML and disdrometer plays a larger role. For instance, the chance for rain at the disdrometer is (naturally) higher for higher temperatures (ca. 5°C) than for lower temperatures (-10°C), even if it may be snowing at the CML location in both cases. Other explanations for the CR method performance decrease 5) we see that the CR method estimates rainfall during the true snow event, lasting from 00:00 to 10:00 on the 19th of December. It also wrongly estimates snowfall before and after the true snowfall event. Thus, while the case study map suggests a better agreement between the CR and disdrometer estimates (Fig. 2), there is still a significant discrepancy between the CR and disdrometer estimates in the hourly time series (Fig. 5). This discrepancy could be due to the spatial difference between the CML and disdrometer or disdrometer misclassification, as discussed above. Another explanation could be that the disdrometers classify wet snow mixed precipitation, such as wet snow, as snow, while the CMLs classify wet snow as rainfall, leading to a misclassification by the CMLs. This phenomenon is clearly observable in Fig. ?? where all events featuring CML overestimation of rainfall amounts coincide with the disdrometer recording snow. A similar pattern is evident in Figure ??, where instances of large CML bias around zero degrees often correspond with the disdrometer measuring snow or a combination of rain and snow. This suggests that events characterized by wet snow are likely to be classified as wet by the CML wet classification method. We

also experimented with other CML wet classification methods and found the same results. This indicates that even if we are able to classify dry snow better using the CMLs and weather radar, we might fail at classifying wet snow. Future work could investigate methods for wet snow detection, for instance, by looking at the during the true snowfall event lasting from 00:00 to 10:00 on the 19th of December (Fig. 5), where the CML estimates a long rainy period and the disdrometer estimates a mixture of rainfall and snow.

4.2 The CR and RT methods classification performance

For snowfall classification at temperatures between -2 and 2 degrees, the CR method holds a slight advantage over the RT method, as reflected in a slightly higher MCC (0.3 vs 0.27) and recall score (0.63 vs 0.61) (Table 3). This indicates that the CR method is slightly better at identifying true snow events (higher recall) while maintaining reliable estimates (equal precision of 0.67). Looking at the confusion matrix for the same temperature interval, we observe that compared to the RT method, the CR method correctly identified 2986 true snowy hours, an increase of 453 hours, while wrongly classifying 3731 hours as snow, an increase of 434 hours (Fig. 9). In other words, the CR method identifies more true snowfall events while also wrongly classifying rainy and dry events as snow. The large number of false snow events, also observable at temperatures above 2 degrees, estimated by CR method might be due to the CML rainfall detection algorithm not being triggered by small rainfall events. At temperatures below -2 degrees (Fig. 6, both the CR and RT method snow classification produced recall scores of 0.65, indicating that the weather radar misses many of the snowfall events recorded by the disdrometers. This could be due to the spatial difference between the ~~radar estimate and the CML estimate or by refining and testing the method proposed by Cherkassky et al. (2014) on a larger dataset~~ CML and disdrometer or disdrometer misclassification, as discussed above. Another explanation could be that blowing winds or road traffic transport snow horizontally, causing the disdrometers to detect snow that does not originate from the sky.

4.3 ~~CMLs improve rainfall detection~~

In terms of rainfall classification, the CR method performs ~~just as well as~~ as well as or outperforms the RT method for all ~~temperature ranges (Fig. 8 and Fig. ??). This~~ temperatures above -2 degrees (Table 3). For instance, for temperatures above 2 degrees, the binary accuracy score for rainfall increases from 0.85 with the RT method to 0.88 with the CR method, and the binary MCC for rainfall increases from 0.34 to 0.52. However, both the RT and CR methods still miss many of the rainfall events observed by the disdrometer, which is evident in their recall scores of 0.66 and 0.77, respectively. As discussed above, this could be due to the fact that the CMLs are located on the ground, which situates them closer to the disdrometers compared to the radar beam. Alternatively, the improved accuracy spatial difference between the CML and disdrometer, or for instance ~~splashing from the roads, leading the disdrometers to estimate rainfall that is not detected by the CML or weather radar. The increased performance of the CR method, compared to the RT method, could be due to radar beam blockage by mountains causing insufficient coverage at some locations. We note that the RT method uses the CML geometry to estimate the radar rainfall and that it could be improved by using the pixel value at the position of the disdrometer. This was done to make the CR overshooting or the radar beam being blocked by mountains.~~

500 4.3 Uncertainties, the impact of the aggregation method and mixed precipitation types

The impact of mixed precipitation, such as wet snow, on the observation methods (disdrometers, CR method, and RT method) remains a significant source of uncertainty in this study. This uncertainty arises from the fact that none of the observation methods can reliably classify mixed precipitation. Additionally, accurately classifying hours that may contain both snow and rain when aggregating the data to hourly intervals poses a challenge. One solution is to introduce a mixed class, classifying hours with both snow and rain as mixed precipitation. However, it remains unclear whether true mixed precipitation, like wet snow, would consistently cause the disdrometer, CR, and RT methods ~~have the same spatial differences as the disdrometer, making them more comparable. Finally, we can also observe that the performance of the~~ to alternate between detecting rain and snow, which could make the mixed class less physically meaningful and lead to inconsistent representations across different estimation methods. While other studies, such as Pickering et al. (2021), aggregated multiple precipitation type data from different sensors to longer periods using a boolean algorithm, we found that the sensors used in our study differed too much for a similar approach. For instance, the RT method uses temperature data with hourly resolution, which complicates accurately capturing hours with both wet and solid precipitation types. While some studies introduce mixed precipitation estimates by classifying precipitation within a fixed temperature interval as mixed (Harpold et al., 2017), the true precipitation type within this interval could still be purely rain or purely snow, leading to inaccurate classifications. Furthermore, since the radar might estimate precipitation slightly before the CML, the CR method is ~~lower at -1 degrees than at 3 degrees (Fig. ??).~~ prone to estimate snow before rainfall events, leading to an overestimation of mixed precipitation. This could be ~~due to the fact that at temperatures below -1 degrees, there are more mixed events where the disdrometer records snow and the CML estimates rainfall~~ addressed by aggregating the CML wet period so that the radar precipitation estimates fall inside the wet period, but this would require further tuning to avoid estimating too many rainfall events at the expense of fewer true mixed events. This work uses a simplified aggregation method in order to avoid introducing too many parameters. We found that, while this approach produces a higher rain to snow ratio for negative temperatures, the assumptions are stated more explicit, and the final results and conclusion remain similar to what we got using other aggregation methods.

520 4.4 ~~Wet snow causes significant discrepancies between CML and radar estimates around zero degrees~~

Around zero degrees~~the CML estimates,~~ the CMLs estimate larger rainfall amounts compared to the weather radar (Fig. ~~??~~). This effect has been observed before in previous studies, for instance in Graf et al. (2020), where the authors noted a marked discrepancy between CML and radar readings during the winter months, potentially induced by wet snow. Many of the significant discrepancies between the radar and CML estimate coincide with hours during which a mix of rain and snow events were recorded (Fig. ~~??~~)-7). The same temperature interval is also characterized by the disdrometers observing both rainfall and snow. This suggests that significant discrepancies between the CML and radar estimates around zero degrees may be attributed to wet snow. ~~From 4°C upwards, both the radar and CMLs provide similar spread in rainfall amount estimates, indicating a balanced comparison at these temperatures. This suggests that there is less discrepancy or bias between CML and radar rainfall rate measurements when the dew point temperature is above 4°C. This effect has been observed before in previous studies, such~~

as Overeem et al. (2016) and Graf et al. (2020), where a marked positive CML bias during the winter months was observed. Further, Fig. 7 reveal that the CML bias as a function of temperature, follows a smooth transition. This indicate that wet snow, as observed by the CML, do not belong to a homogeneous group, but instead follow a gradual transition from snow to rainfall while melting.

4.4 Nearby CMLs can be used to interpret road friction

In Fig. ?? we can observe that strong snow events causes the road friction to drop. This occurs, for instance, around the 12th, when the disdrometer observes snow. The strongest drop in road friction appears to coincide with instances where both the CML indicates rainfall and While studies such as Gjertsen and Ødegaard (2005), Casellas et al. (2021), and Saltikoff et al. (2015) have evaluated the performance of temperature-based precipitation phase classification methods, these studies typically vary in methodology, terrain complexity, radar technology, and the instruments used to estimate the ground truth. This variability introduces challenges when comparing results across different studies. Although the disdrometers used in this study provide a large dataset, they have some limitations; in particular, the disdrometer registers snow. During these events there is also a significant discrepancy between the weather radar and the CML estimates. This discrepancy can, as previously discussed, be caused by wet snow, suggesting that the pronounced decrease in road friction might be attributed to conditions of wet snow. However, for practical applications, it must be noted that road friction can also drop due to other factors, such as icy roads large number of rainy events recorded below zero degrees and the lack of mixed class classification introduce uncertainties specific to this study. Further, any type of wet precipitation can cause the CML signal level to drop, potentially leading to precipitation being falsely classified as rainfall. Another source of uncertainty is the spatial distance between the disdrometer and the CML, where for instance temperature variations due to elevation and spatial differences can affect precipitation classification. Moreover, we can also observe that not all wet snow periods cause the road friction to drop. Reasons for this could be, for instance, that water on the road is causing wet snow to melt, a too short duration of the snow event, or that the snow was removed by the road authorities the temperature model used is based on model data, and could be improved by using ground based sensors. Combined, these factors introduce large uncertainties in this study, and further make it challenging to directly compare the CR and RT estimates in this study to those from similar studies.

Nevertheless, our study demonstrates that CMLs can be used to enhance classification of snow and rainfall around zero degrees, which are useful for hydrological applications such as in predicting hydropower production, flooding, avalanches and slush avalanches.

5 Conclusions

In this work, we have compared two methods for classifying rain and snow, one established reference method where we combine surface dew point temperature and weather radar. The "radar-temperature" (RT) and one novel method where we combine CMLs and weather radar (CR). The CR method works by classifying weather radar precipitation below zero degrees as snow and above as rain, using dew-point temperature derived from downscaled ERA5 data. The "CML-radar" (CR) method,

565 exploits the fact that dry snow causes ~~low signal attenuation of minimal signal attenuation in~~ the CML signal level, ~~making~~
~~dry snow events appear similar to dry events in the CML time series. It and~~ works by classifying time steps where the weather
radar detects precipitation, and the CMLs do not detect precipitation, ~~as snowy~~. Time steps where the CML detects rainfall
are set to ~~wet. The RT method classifies weather radar precipitation below zero degrees as snow and above as rain. rainy. The~~
~~estimates were compared to estimates from nearby disdrometers located along roads in Norway.~~

570 Our results show that the CR method outperforms the RT method for dry snow detection ~~above zero between -2 and 2~~ degrees
and, in general, for rainfall detection, suggesting that CMLs can be used to better classify rain and snow. Further, our results
indicate that wet snow is classified as rainfall by the ~~CML CMLs~~ and that during these events the ~~disdrometer disdrometers~~
tends to estimate a mix of rainfall and snow. ~~These events are also characterized by large CML overestimations compared to~~
~~radar, which could be attributed to the larger signal attenuation caused by wet snow. Future work should investigate methods~~
575 ~~for CML wet snow detection, preferably using several different precipitation type sensors as ground truth, as suggested by~~
~~Pickering et al. (2021). Future work should also investigate how the CR estimates impact hydrological models.~~

Overall, our findings suggest a new application for using CMLs to identify dry snow and contribute to better understanding
on how CMLs behave during events of mixed precipitation.

Code and data availability. The software used for CML processing software is available under [https://github.com/pycomlink/pycomlink/](https://github.com/pycomlink/pycomlink/tree/master)
580 [tree/master](https://github.com/pycomlink/pycomlink/tree/master). Disdrometer data is available from (Frost, 2024). Radar data is available from (THREDDS, 2024). CML data were provided by
Ericsson and are not publicly available.

Author contributions. Conceptualization: EØ, JA, RB. Data curation: EØ. Methodology: EØ, JA, RG, RB, MW, NOK, CC, VN. Software:
EØ, CC. Supervision: VN, MW, NOK, RB. Writing – original draft preparation: EØ. Writing – review and editing: EØ, RG, JA, RB, MW,
NOK, CC, VN.

585 *Competing interests.* The contact author has declared that neither of the authors has any competing interests.

Acknowledgements. The authors thank co-supervisor Etienne Leblois for nice discussions. We would also like to thank Ericsson for providing
CML data. This work is funded by the Norwegian University of Life Sciences and the German Research Foundation via the SpraiLINK
project (Grant CH-1785/2-1).

References

- 590 Berne, A. and Krajewski, W.: Radar for hydrology: Unfulfilled promise or unrecognized potential?, *Advances in Water Resources*, 51, 357–366, <https://doi.org/10.1016/j.advwatres.2012.05.005>, 2013.
- Blettner, N., Fencel, M., Bareš, V., Kunstmann, H., and Chwala, C.: Transboundary Rainfall Estimation Using Commercial Microwave Links, *Earth and Space Science*, 10, <https://doi.org/10.1029/2023EA002869>, 2023.
- Bloemink, H.: Precipitation type from the Thies disdrometer, in: WMO Tech. Conf. on Meteorological and Environmental Instruments and
595 Methods of Observation (TECO-2005), pp. 1–7, World Meteorological Organization, Bucharest, Romania, https://library.wmo.int/viewer/41919/download?file=wmo-td_1265.pdf&type=pdf&navigator=1, accessed: 2025-01-23, 2005.
- Casellas, E., Bech, J., Veciana, R., Pineda, N., Miró, J. R., Moré, J., Rigo, T., and Sairouni, A.: Nowcasting the precipitation phase combining weather radar data, surface observations, and NWP model forecasts, *Quarterly Journal of the Royal Meteorological Society*, 147, 3135–3153, <https://doi.org/10.1002/qj.4121>, 2021.
- 600 Chandrasekar, V., Keränen, R., Lim, S., and Moisseev, D.: Recent advances in classification of observations from dual polarization weather radars, *Atmospheric Research*, 119, 97–111, <https://doi.org/10.1016/j.atmosres.2011.08.014>, 2013.
- Cherkassky, D., Ostrometzky, J., and Messer, H.: Precipitation Classification Using Measurements From Commercial Microwave Links, *IEEE Transactions on Geoscience and Remote Sensing*, 52, 2350–2356, <https://doi.org/10.1109/TGRS.2013.2259832>, 2014.
- Chicco, D. and Jurman, G.: The advantages of the Matthews correlation coefficient (MCC) over F1 score and accuracy in binary classification
605 evaluation, *BMC Genomics*, 21, 6, <https://doi.org/10.1186/s12864-019-6413-7>, 2020.
- Chwala, C., Polz, J., Graf, M., Sereb, D., Blettner, N., Keis, F., and Boose, Y.: pycomlink/pycomlink: v0.3.2, <https://doi.org/https://doi.org/10.5281/zenodo.4810169>, 2023.
- Elmore, K. L.: The NSSL Hydrometeor Classification Algorithm in Winter Surface Precipitation: Evaluation and Future Development, *Weather and Forecasting*, 26, 756–765, <https://doi.org/10.1175/WAF-D-10-05011.1>, 2011.
- 610 Feiccabrino, J. M.: Precipitation phase uncertainty in cold region conceptual models resulting from meteorological forcing time-step intervals, *Hydrology Research*, 51, 180–187, <https://doi.org/10.2166/nh.2020.080>, 2020.
- Friedrich, K., Kalina, E. A., Masters, F. J., and Lopez, C. R.: Drop-Size Distributions in Thunderstorms Measured by Optical Disdrometers during VORTEX2, *Monthly Weather Review*, 141, 1182–1203, <https://doi.org/10.1175/MWR-D-12-00116.1>, 2013.
- Frost: <https://frost.met.no/index.html>, 2024.
- 615 Førland, E., Allerup, P., Dahlström, B., Elomaa, E., Jónsson, T., Madsen, H., Perälä, J., Rissanen, P., Vedin, H., and Vejen, F.: Manual for Operational Correction of Nordic Precipitation Data, DNMI-report, Norske meteorologiske institutt, <https://books.google.no/books?id=HLIKcgAACAAJ>, 1996.
- Gjertsen, U. and Ødegaard, V.: The water phase of precipitation—a comparison between observed, estimated and predicted values, *Atmospheric Research*, 77, 218–231, <https://doi.org/10.1016/j.atmosres.2004.10.030>, 2005.
- 620 Gorodkin, J.: Comparing two K-category assignments by a K-category correlation coefficient, *Computational Biology and Chemistry*, 28, 367–374, <https://doi.org/10.1016/j.compbiolchem.2004.09.006>, 2004.
- Graf, M., Chwala, C., Polz, J., and Kunstmann, H.: Rainfall estimation from a German-wide commercial microwave link network: optimized processing and validation for 1 year of data, *Hydrology and Earth System Sciences*, 24, 2931–2950, <https://doi.org/10.5194/hess-24-2931-2020>, 2020.

- 625 Grazioli, J., Tuia, D., and Berne, A.: Hydrometeor classification from polarimetric radar measurements: a clustering approach, *Atmospheric Measurement Techniques*, 8, 149–170, <https://doi.org/10.5194/amt-8-149-2015>, 2015.
- Hansryd, J., Li, Y., Chen, J., and Ligander, P.: Long term path attenuation measurement of the 71–76 GHz band in a 70/80 GHz microwave link, in: *Proceedings of the Fourth European Conference on Antennas and Propagation*, pp. 1–4, 2010.
- Harder, P. and Pomeroy, J.: Estimating precipitation phase using a psychrometric energy balance method, *Hydrological Processes*, 27, 1901–
- 630 1914, <https://doi.org/10.1002/hyp.9799>, 2013.
- Harder, P. and Pomeroy, J. W.: Hydrological model uncertainty due to precipitation-phase partitioning methods, *Hydrological Processes*, 28, 4311–4327, <https://doi.org/10.1002/hyp.10214>, 2014.
- Harpold, A. A., Kaplan, M. L., Klos, P. Z., Link, T., McNamara, J. P., Rajagopal, S., Schumer, R., and Steele, C. M.: Rain or snow: hydrologic processes, observations, prediction, and research needs, *Hydrology and Earth System Sciences*, 21, 1–22, [https://doi.org/10.5194/hess-21-](https://doi.org/10.5194/hess-21-1-2017)
- 635 1-2017, 2017.
- Hestnes, E.: A Contribution to the Prediction of Slush Avalanches, *Annals of Glaciology*, 6, 1–4, <https://doi.org/10.3189/1985AoG6-1-1-4>, 1985.
- ITU, R.: RECOMMENDATION ITU-R P.838-3 Specific attenuation model for rain for use in prediction methods, pp. 1–8, 2005.
- Jennings, K. S., Winchell, T. S., Livneh, B., and Molotch, N. P.: Spatial variation of the rain–snow temperature threshold across the Northern
- 640 Hemisphere, *Nature Communications*, 9, 1148, <https://doi.org/10.1038/s41467-018-03629-7>, 2018.
- Jurman, G., Riccadonna, S., and Furlanello, C.: A Comparison of MCC and CEN Error Measures in Multi-Class Prediction, *PLoS ONE*, 7, e41882, <https://doi.org/10.1371/journal.pone.0041882>, 2012.
- Kienzie, S. W.: A new temperature based method to separate rain and snow, *Hydrological Processes*, 22, 5067–5085, <https://doi.org/10.1002/hyp.7131>, 2008.
- 645 Kochendorfer, J., Earle, M., Rasmussen, R., Smith, C., Yang, D., Morin, S., Mekis, E., Buisan, S., Roulet, Y.-A., Landolt, S., Wolff, M., Hoover, J., Thériault, J. M., Lee, G., Baker, B., Nitu, R., Lanza, L., Colli, M., and Meyers, T.: How Well Are We Measuring Snow Post-SPICE?, *Bulletin of the American Meteorological Society*, 103, E370–E388, <https://doi.org/10.1175/BAMS-D-20-0228.1>, 2022.
- Kuhn, M.: Micro-Meteorological Conditions for Snow Melt, *Journal of Glaciology*, 33, 24–26, <https://doi.org/10.3189/S002214300000530X>, 1987.
- 650 Lamb, D. and Verlinde, J.: *Physics and Chemistry of Clouds*, Cambridge University Press, ISBN 9780521899109, <https://doi.org/10.1017/CBO9780511976377>, 2011.
- Lawrence, M. G.: The Relationship between Relative Humidity and the Dewpoint Temperature in Moist Air: A Simple Conversion and Applications, *Bulletin of the American Meteorological Society*, 86, 225–234, <https://doi.org/10.1175/BAMS-86-2-225>, 2005.
- Leijnse, H., Uijlenhoet, R., and Stricker, J. N. M.: Rainfall measurement using radio links from cellular communication networks, *Water*
- 655 *Resources Research*, 43, 1–6, <https://doi.org/10.1029/2006WR005631>, 2007.
- Leijnse, H., Uijlenhoet, R., and Stricker, J.: Microwave link rainfall estimation: Effects of link length and frequency, temporal sampling, power resolution, and wet antenna attenuation, *Advances in Water Resources*, 31, 1481–1493, <https://doi.org/10.1016/j.advwatres.2008.03.004>, 2008.
- Leroux, N. R., Vionnet, V., and Thériault, J. M.: Performance of precipitation phase partitioning methods and their impact on snowpack
- 660 evolution in a humid continental climate, *Hydrological Processes*, 37, <https://doi.org/10.1002/hyp.15028>, 2023.
- Loth, B., Graf, H., and Oberhuber, J. M.: Snow cover model for global climate simulations, *Journal of Geophysical Research: Atmospheres*, 98, 10 451–10 464, <https://doi.org/10.1029/93JD00324>, 1993.

- Lussana, C., Seierstad, I. A., Nipen, T. N., and Cantarello, L.: Spatial interpolation of two-metre temperature over Norway based on the combination of numerical weather prediction ensembles and in situ observations, *Quarterly Journal of the Royal Meteorological Society*, 145, 3626–3643, <https://doi.org/10.1002/qj.3646>, 2019.
- Lussana, C., Nipen, T. N., Seierstad, I. A., and Elo, C. A.: Ensemble-based statistical interpolation with Gaussian anamorphosis for the spatial analysis of precipitation, *Nonlinear Processes in Geophysics*, 28, 61–91, <https://doi.org/10.5194/npg-28-61-2021>, 2021.
- Löffler-Mang, M. and Joss, J.: An Optical Disdrometer for Measuring Size and Velocity of Hydrometeors, *Journal of Atmospheric and Oceanic Technology*, 17, 130–139, [https://doi.org/10.1175/1520-0426\(2000\)017<0130:AODFMS>2.0.CO;2](https://doi.org/10.1175/1520-0426(2000)017<0130:AODFMS>2.0.CO;2), 2000.
- Marks, D., Winstral, A., Reba, M., Pomeroy, J., and Kumar, M.: An evaluation of methods for determining during-storm precipitation phase and the rain/snow transition elevation at the surface in a mountain basin, *Advances in Water Resources*, 55, 98–110, <https://doi.org/10.1016/j.advwatres.2012.11.012>, 2013.
- Marshall, J. S. and Palmer, W. M. K.: The distribution of raindrops with size, *Journal of Meteorology*, 5, 165–166, [https://doi.org/10.1175/1520-0469\(1948\)005<0165:TDORWS>2.0.CO;2](https://doi.org/10.1175/1520-0469(1948)005<0165:TDORWS>2.0.CO;2), 1948.
- Matsuo, T., Sasyo, Y., and Sato, Y.: Relationship between Types of Precipitation on the Ground and Surface Meteorological Elements, *Journal of the Meteorological Society of Japan. Ser. II*, 59, 462–476, https://doi.org/10.2151/jmsj1965.59.4_462, 1981.
- McCabe, G. J., Clark, M. P., and Hay, L. E.: Rain-on-Snow Events in the Western United States, *Bulletin of the American Meteorological Society*, 88, 319–328, <https://doi.org/10.1175/BAMS-88-3-319>, 2007.
- Messer, H., Zinevich, A., and Pinhas, A.: Environmental Monitoring by Wireless Communication Networks, *Science*, 312, 17–18, <https://www.jstor.org/stable/3846088>, 2006.
- MET: MET Nordic dataset, <https://github.com/metno/NWPdocs/wiki/MET-Nordic-dataset>, 2024.
- Nešpor, V. and Sevruck, B.: Estimation of Wind-Induced Error of Rainfall Gauge Measurements Using a Numerical Simulation, *Journal of Atmospheric and Oceanic Technology*, 16, 450–464, [https://doi.org/10.1175/1520-0426\(1999\)016<0450:EOWIEO>2.0.CO;2](https://doi.org/10.1175/1520-0426(1999)016<0450:EOWIEO>2.0.CO;2), 1999.
- Ostrometzky, J., Cherkassky, D., and Messer, H.: Accumulated Mixed Precipitation Estimation Using Measurements from Multiple Microwave Links, *Advances in Meteorology*, 2015, 1–9, <https://doi.org/10.1155/2015/707646>, 2015.
- Overeem, A., Leijnse, H., and Uijlenhoet, R.: Measuring urban rainfall using microwave links from commercial cellular communication networks, *Water Resources Research*, 47, <https://doi.org/10.1029/2010WR010350>, 2011.
- Overeem, A., Leijnse, H., and Uijlenhoet, R.: Country-wide rainfall maps from cellular communication networks, *Proceedings of the National Academy of Sciences*, 110, 2741–2745, <https://doi.org/10.1073/pnas.1217961110>, 2013.
- Overeem, A., Leijnse, H., and Uijlenhoet, R.: Two and a half years of country-wide rainfall maps using radio links from commercial cellular telecommunication networks, *Water Resources Research*, 52, 8039–8065, <https://doi.org/10.1002/2016WR019412>, 2016.
- Pastorek, J., Fencel, M., and Bareš, V.: Uncertainties in discharge predictions based on microwave link rainfall estimates in a small urban catchment, *Journal of Hydrology*, 617, 129 051, <https://doi.org/10.1016/j.jhydrol.2022.129051>, 2023.
- Paulson, K. and Al-Mreri, A.: A rain height model to predict fading due to wet snow on terrestrial links, *Radio Science*, 46, <https://doi.org/10.1029/2010RS004555>, 2011.
- Pedregosa, F., Varoquaux, G., Gramfort, A., Michel, V., Thirion, B., Grisel, O., Blondel, M., Prettenhofer, P., Weiss, R., Dubourg, V., Vanderplas, J., Passos, A., Cournapeau, D., Brucher, M., Perrot, M., and Duchesnay, E.: Scikit-learn: Machine Learning in Python, *Journal of Machine Learning Research*, 12, 2825–2830, 2011.

- Pickering, B. S., Neely, R. R., Jeffery, J., Dufton, D., and Lukach, M.: Evaluation of Multiple Precipitation Sensor Designs for Precipitation Rate and Depth, Drop Size and Velocity Distribution, and Precipitation Type, *Journal of Hydrometeorology*, 22, 703–720, <https://doi.org/10.1175/JHM-D-20-0094.1>, 2021.
- poligrain: Poligrain, <https://github.com/OpenSenseAction/poligrain>, 2024.
- Polz, J., Chwala, C., Graf, M., and Kunstmann, H.: Rain event detection in commercial microwave link attenuation data using convolutional neural networks, *Atmospheric Measurement Techniques*, 13, 3835–3853, <https://doi.org/10.5194/amt-13-3835-2020>, 2020.
- Pu, K., Liu, X., Hu, S., and Gao, T.: Hydrometeor Identification Using Multiple-Frequency Microwave Links: A Numerical Simulation, *Remote Sensing*, 12, 2158, <https://doi.org/10.3390/rs12132158>, 2020.
- Saltikoff, E., Lopez, P., Taskinen, A., and Pulkkinen, S.: Comparison of quantitative snowfall estimates from weather radar, rain gauges and a numerical weather prediction model, *Boreal Environment Research*, 20, 2015.
- Schleiss, M., Rieckermann, J., and Berne, A.: Quantification and Modeling of Wet-Antenna Attenuation for Commercial Microwave Links, *IEEE Geoscience and Remote Sensing Letters*, 10, 1195–1199, <https://doi.org/10.1109/LGRS.2012.2236074>, 2013.
- Stewart, R. E.: Precipitation Types in the Transition Region of Winter Storms, *Bulletin of the American Meteorological Society*, 73, 287–296, [https://doi.org/10.1175/1520-0477\(1992\)073<0287:PTITTR>2.0.CO;2](https://doi.org/10.1175/1520-0477(1992)073<0287:PTITTR>2.0.CO;2), 1992.
- Stewart, R. E., Thériault, J. M., and Henson, W.: On the Characteristics of and Processes Producing Winter Precipitation Types near 0°C, *Bulletin of the American Meteorological Society*, 96, 623–639, <https://doi.org/10.1175/BAMS-D-14-00032.1>, 2015.
- THREDDS: <https://thredds.met.no/thredds/catalog.html>, 2024.
- van Leth, T. C., Overeem, A., Leijnse, H., and Uijlenhoet, R.: A measurement campaign to assess sources of error in microwave link rainfall estimation, *Atmospheric Measurement Techniques*, 11, 4645–4669, <https://doi.org/10.5194/amt-11-4645-2018>, 2018.
- Wolff, M. A., Isaksen, K., Petersen-Øverleir, A., Ødemark, K., Reitan, T., and Brækkan, R.: Derivation of a new continuous adjustment function for correcting wind-induced loss of solid precipitation: results of a Norwegian field study, *Hydrology and Earth System Sciences*, 19, 951–967, <https://doi.org/10.5194/hess-19-951-2015>, 2015.
- Yuter, S. E., Kingsmill, D. E., Nance, L. B., and Löffler-Mang, M.: Observations of Precipitation Size and Fall Speed Characteristics within Coexisting Rain and Wet Snow, *Journal of Applied Meteorology and Climatology*, 45, 1450–1464, <https://doi.org/10.1175/JAM2406.1>, 2006.
- Øydvin, E., Graf, M., Chwala, C., Wolff, M. A., Kitterød, N.-O., and Nilsen, V.: Technical Note: A simple feedforward artificial neural network for high temporal resolution classification of wet and dry periods using signal attenuation from commercial microwave links, *EGUsphere* [preprint], <https://doi.org/https://doi.org/10.5194/egusphere-2024-647>, 2024.